Substrate-dependent allosteric regulation by switchable catalytic molecular tweezers

Lorien Benda, Benjamin Doistau, Caroline Rossi-Gendron, Lise-Marie Chamoreau, Bernold Hasenknopf, Guillaume Vives

COMMUNICATIONS CHEMISTRY

ARTICLE

https://doi.org/10.1038/s42004-019-0246-9 OPEN

Substrate-dependent allosteric regulation by switchable catalytic molecular tweezers

Lorien Benda[1], Benjamin Doistau[1], Caroline Rossi-Gendron[1], Lise-Marie Chamoreau[1], Bernold Hasenknopf[1] & Guillaume Vives[1*]

Allosteric regulation is exploited by biological systems to regulate the activity and/or selectivity of enzymatic reactions but remains a challenge for artificial catalysts. Here we report switchable terpy(Zn-salphen)$_2$ molecular tweezers and their metal-dependent allosteric regulation of the acetylation of pyridinemethanol isomers. Zinc-salphen moieties can both act as a Lewis acid to activate the anhydride reagents and provide a binding site for pyridinemethanol substrates. The tweezers' conformation can be reversibly switched between an open and a closed form by a metal ion stimulus. Both states offer distinct catalytic profiles, with closed tweezers showing superior catalytic activity towards *ortho* substrates, while open tweezers presenting higher rate for the acetylation of *meta* and *para* substrates. This notable substrate dependent allosteric response is rationalized by a combination of experimental results and calculations supporting a bimetallic reaction in the closed form for *ortho* substrate and an inhibition of the cavity for *meta* and *para* substrates.

[1] Sorbonne Université, CNRS UMR8232, Institut Parisien de Chimie Moléculaire, 4 place Jussieu, 75005 Paris, France. *email: guillaume.vives@sorbonne-universite.fr

Understanding and harnessing the mechanical motion of chemical systems are a significant endeavor of supramolecular chemistry[1–3]. Recent advances in the field have led to the design and synthesis of increasingly complex molecular switches[4] and machines[5–10]. While the control of motion at the molecular level has been mastered in some architectures, exploiting such movement to produce useful tasks remains a challenge. Nature already uses mechanical motion to regulate the activity and/or selectivity of enzymatic reactions by allosteric effects. Inspired by such sophisticated machinery, artificial switchable catalysts where the rate or outcome of chemical transformations can be controlled by external stimuli have recently received great interest[11–15]. Photoswitchable catalytic systems have been developed to harness the steric and/or electronic changes resulting from the photoisomerization of azobenzene[16–19], photochromic[20], or motor[21,22] derivatives. Rotaxane-based switchable catalysts have been developed using the motion of a macrocycle to reveal or hide catalytic sites on the thread in response to a chemical stimulus[23–27]. More complex interlocked architectures such as molecular knots[28] have also been reported to display allosteric regulation. Coordination-based mechanical switches are attractive as they allow addressability by the design of the coordination sites and afford thermal stability and total conversion between the states[29–35]. Some examples of allosteric regulation using coordination-based mechanical switches have been described[36–42]. In particular, Mirkin has developed a "weak-link" approach to construct a variety of addressable and conformationally flexible entities capable of catalyzing reactions with allosteric enzyme-like control[43–47]. While significant advances have been made in the development of switchable catalysts, achieving substrate-dependent regulations remains a challenge[48].

Among switchable mechanical systems, switchable molecular tweezers[49–52] offer the possibility of coupling mechanical function and chemical activity, thus paving the way towards supramolecular smart catalysts. We have designed switchable molecular tweezers using metal coordination to control properties at the molecular level by mechanical motion. These tweezers are composed of two moieties: (i) a central terpyridine ligand substituted in 6 and 6" positions as switchable unit and (ii) two M-salphen complexes as functional units. The terpyridine ligand can reversibly transition from an open W shaped form to a closed U shaped geometry upon metal coordination (Fig. 1). Closure of the tweezers brings in close spatial proximity the two salphen moieties, thus creating a cavity suitable for host–guest interactions. The versatility of our system and the drastic and controlled modification of the distance between the two functional units has been successfully applied to modulate luminescent[53–55], magnetic[56,57], or redox properties[58] using Pt(II), Cu(II), and Ni (II) salphen complexes, respectively. We wished to further exploit the modularity of our platform to obtain a catalytic system that can be controlled by a mechanical motion by analogy with the activity of enzymes that are often modulated by cofactors or allosteric regulation. A key feature of this approach is that the allosteric binding event causes a structural change of the entire molecule by generating an active site upon closing with a potential cooperative double activation from the two M-salphen units in close proximity. Acyl-transfer reaction with pyridinemethanol substrates was chosen as a benchmark reaction since it has been previously used by Sanders[59] to demonstrate supramolecular catalysis in Zn-porphyrin cages and later by Mirkin[46,60,61] to evaluate allosteric regulation.

Herein we present the synthesis and reversible switching of terpy(Zn-salphen)$_2$ tweezers **1** as well as their switchable catalytic activity with substrate-dependent allosteric regulation in the acetylation of pyridinemethanol derivatives. Closed tweezers present superior catalytic activity towards *ortho* substrates, while open tweezers present higher rate for the acetylation of *meta* and *para* substrates. This substrate-dependent allosteric response is rationalized by a combination of experimental results and density functional theory (DFT) calculations supporting a bimetallic reaction in the closed form for *ortho* substrate and an inhibition of the cavity for *meta* and *para* substrates.

Results and discussion

Synthesis. Tweezers **1** were synthesized by a Zn(II)-templated reaction[62,63] between hemi-salphen **7**[64] and hemi-tweezers **6** as key step (Fig. 2). 3-(tert-butyl)-2-hydroxybenzaldehyde was first regioselectively iodinated[65] in position 5 thanks to the strong *para* activating effect of the phenol group. **2** was then subjected to a Sonogashira coupling reaction with trimethylsilylacetylene (TMSA) to obtain the protected alkyne **3**[66,67]. After deprotection with TBAF in THF, **4**[67] was reacted with dibromo-terpyridine **5** in double Sonogashira coupling reaction to yield hemi-tweezers **6**. In the final step, zinc acetate was used as template[62] for the formation of the salphen moieties between **6** and hemi-salphen **7** by reaction at room temperature in methanol in the presence of NEt_3. Closed [Zn(**1**)](OAc)$_2$ tweezers were obtained in 80% yield after recrystallization in acetonitrile. This Zn-templated reaction enabled the formation of the dissymmetric salphen moieties in a good yield by stabilizing the imine bond of preformed hemi-salphen **7** and avoiding a scrambling between the salicylaldehyde fragments. The structure was characterized by NMR spectroscopy (see Supplementary Fig. 30–34) and mass spectrometry with a signal at *m/z* 1496.45 corresponding to mono-charged [Zn(**1**)OAc]$^+$ species.

Single crystals of [Zn(**1**)](OAc)$_2$ suitable for X-ray diffraction were obtained by slow evaporation of a MeOH/$CHCl_3$ mixture (Fig. 3). The closed tweezers crystallize in trigonal space group R-3 in a unit cell of 49749 Å^3 ($a = 44.1588(14)$ Å; $b = 44.1588(14)$ Å; $c = 29.4589(10)$ Å; $\alpha = \beta = 90°$; $\gamma = 120°$). In the solid state, the tweezers appear as a head to tail dimer around an inversion center with two bridging hydroxyl groups connecting a zinc of one salphen moiety of one tweezers to the zinc coordinated to the terpyridine unit of the second one, and *vice versa*. For both tweezers, the phenylene moieties of the two Zn-salphen are located on the same side in a *syn* conformation generating a cavity with an intramolecular Zn–Zn distance of 4.79 Å. The zinc atoms coordinated to the salphen ligands adopt a distorted square pyramidal geometry with apical oxygen atoms from water or hydroxyl ligands at Zn–O distances of 2.046 and 1.957 Å, respectively. In both cases, the Zn atoms are located above the average N_2O_2 plane of the ligand (0.66 and 0.41 Å) with average Zn–O, Zn–N distances of 1.961 Å and 2.076 Å, respectively, in agreement with previously reported Zn-salphen complexes[68–70]. The packing of the tweezers generated large channels with disordered solvent molecules that could not be successfully modeled resulting in a rather high *R* factor (10.9%). By changing the crystallization conditions (slow evaporation of a MeOH/CH_2Cl_2 mixture in the presence of chloride) a structure of closed tweezers with a mixture of acetate and chloride ligands was obtained with a better agreement factor ($R = 6.1\%$). The tweezers adopt the same dimeric conformation with almost identical distances fully validating the previous structure (see Supplementary Fig. 1 and Supplementary Tables 1, 2).

The opening of the tweezers was then investigated by using a competitive ligand with a higher binding constant than terpyridine. In non-coordinating solvents, the ^{1}H NMR signals of the tweezers or simple Zn-salphen complex **9** are usually broad[71–73] probably due to ligand exchange in the apical position of the Zn or some aggregation by the interaction between Zn-salphen moieties (see Supplementary Fig. 2). The addition of a small percentage of

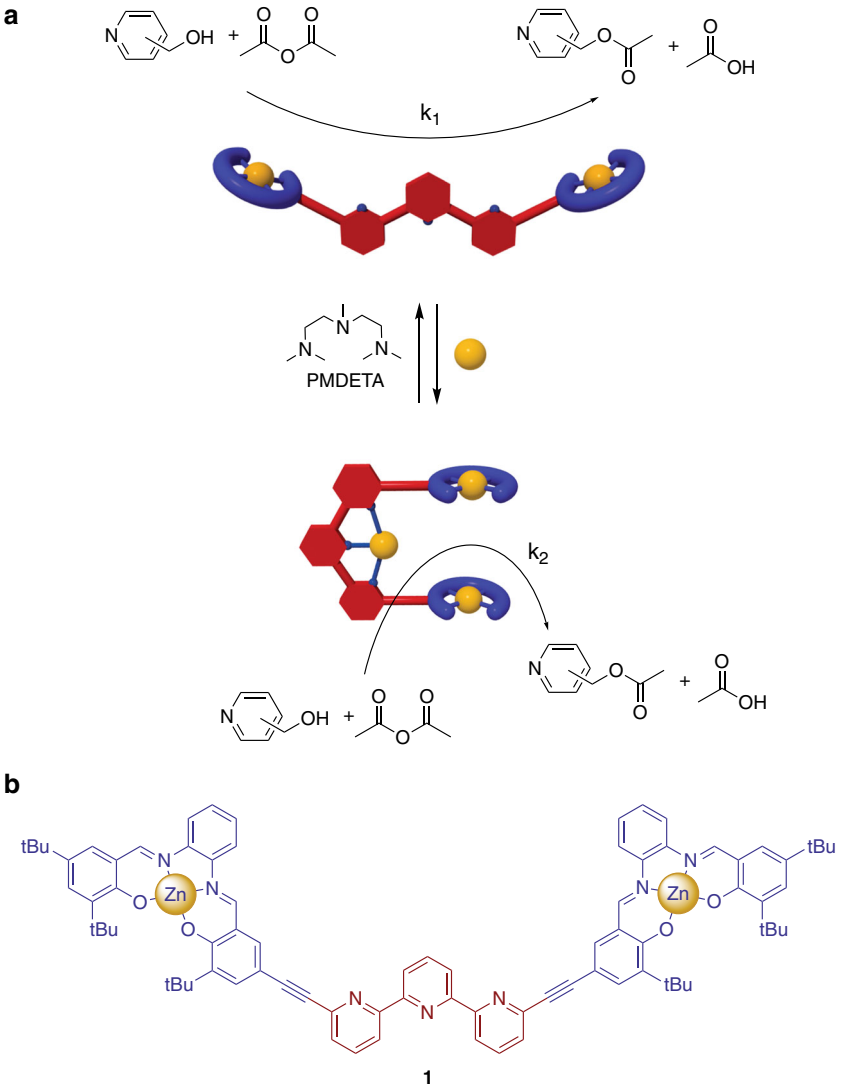

Fig. 1 Catalytic allosteric regulation by switchable molecular tweezers. a Principle of the switching between open and closed conformation of the tweezers to regulate the activity of acyl-transfer reaction. **b** structure of terpy(Zn-salphen)$_2$ tweezers. PMDETA = *N*,*N*,*N*′,*N*″,*N*″-pentamethyldiethylenetriamine.

coordinating solvent such as CD_3OD or THF-d_8 enabled a sharpening of the signals due to the stiffening of the Zn-salphen moieties by the solvent coordination in apical position. The opening was thus monitored by ^{1}H NMR titration (Fig. 4) in a mixture of $CDCl_3$ and MeOD (85/15). Upon addition of *N*,*N*,*N*′,*N*″,*N*″-pentamethyl-diethylenetriamine (PMDETA), we observed a progressive disappearance of the closed tweezers signals and the appearance of a new set of peaks corresponding to the open conformation in slow exchange on the NMR time scale. The conversion can be clearly followed by the appearance of the deshielded imine protons at 8.7 ppm. Since PMDETA forms a 2:1 $[Zn(PMEDTA)_2]^{2+}$ complex with zinc, about three equivalents were necessary to fully open the tweezers. No intermediate bis-terpyridine $[Zn(\mathbf{1})_2]^{2+}$ species was observed during the NMR titration. This was confirmed by an UV-Vis titration (see Supplementary Fig. 4) presenting an isosbestic point at 485 nm in agreement with an equilibrium between only two species closed and open tweezers. Open tweezers **1** were obtained on a preparative scale after purification on LH-20 Sephadex column eluting with THF and were fully characterized by 2D NMR spectroscopy and mass spectrometry. The open W shaped conformation of **1** was confirmed by ^{1}H 1D NOE experiments with the absence of correlation between H-2 and H-3 (see Supplementary Fig. 3).

Switching mechanism. The reversible mechanical motion of the tweezers with $ZnCl_2$ as zinc source was also monitored by NMR (see Supplementary Fig. 5). The addition of one equivalent of $ZnCl_2$ resulted in the tweezers' closing with the formation of the 1:1 complex $[Zn(\mathbf{1})]Cl_2$. This complex was confirmed by mass spectrometry with a signal at *m/z* 1474.41 corresponding to mono-charged $[Zn(\mathbf{1})Cl]^+$ species (see Supplementary Fig. 6). The reversibility of the motion was then achieved by adding 3 equivalents of PMDETA as a competitive ligand with the recovery of the NMR spectra of the open tweezers and a mass signal at *m/z* 1374.51 corresponding to $[\mathbf{1} + H]^+$ (see Supplementary Fig. 7). Three successive closing/opening cycles were achieved on the same sample (see Supplementary Fig. 5) demonstrating the reversible mechanical motion of tweezers by successive coordination and decoordination.

Allosteric regulation studies. We wished to exploit the drastic change in the Zn–Zn distance between the open and closed conformations to regulate the catalytic activity of the tweezers. As a proof of concept, an acyl-transfer reaction between pyridinemethanol isomers and acetic anhydride was used as a benchmark reaction[59,60,74,75]. We hypothesized that a switch

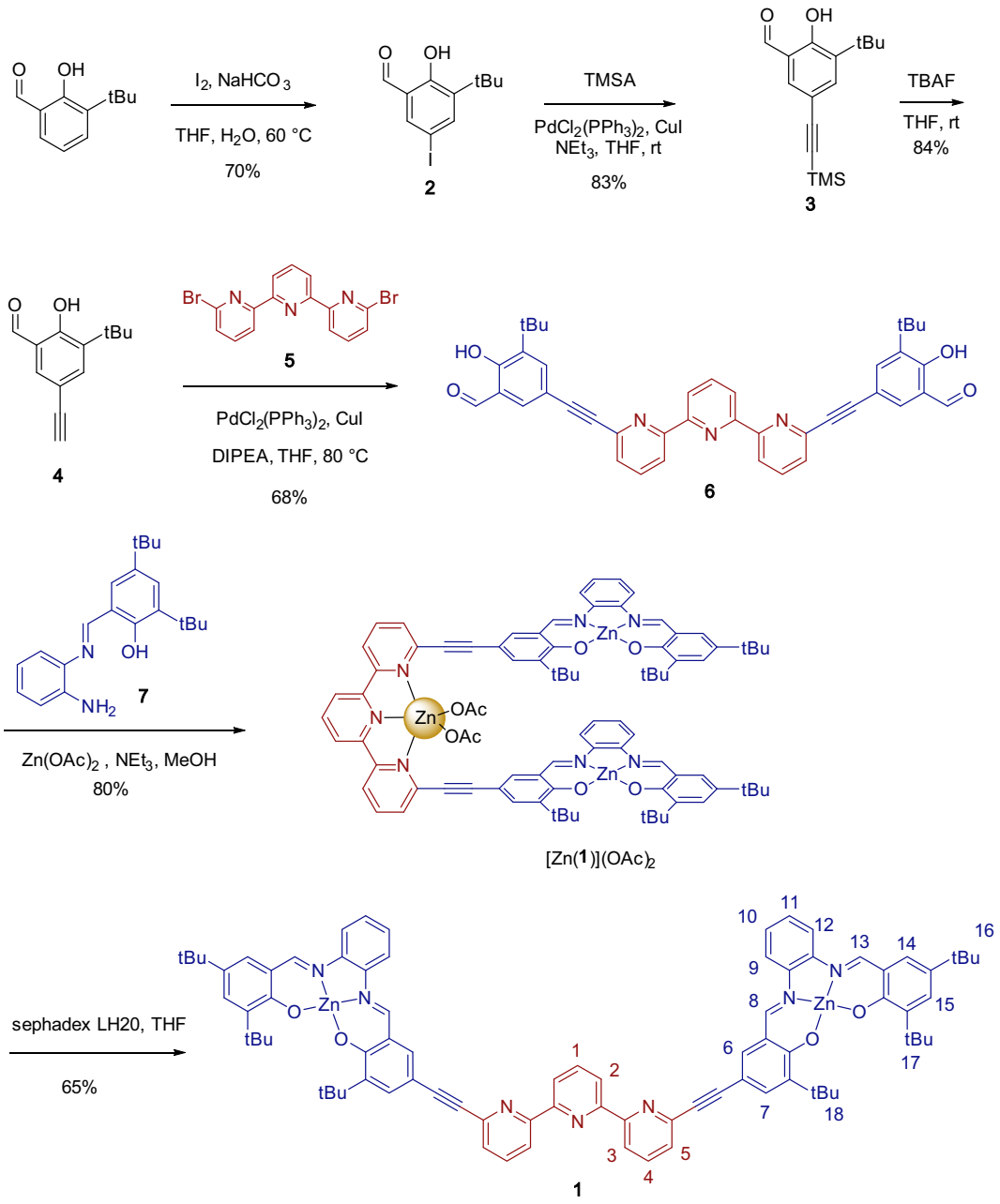

Fig. 2 Synthesis of tweezers 1. Multistep synthesis of Tweezers **1** using Zn(II)-templated reaction as key step.

between the open and the closed conformations should modify the rate of the acyl transfer by switching from a monometallic to a bimetallic activation, respectively. Indeed, in the closed conformation we can expect to bring in proximity both reagents by coordination to the two Zn-salphen moieties as shown by Sanders in porphyrin trimers[59]. The reactions were performed in CD_2Cl_2/THF-d_8 (95/5) at 300 K with 14 mol% catalyst and monitored by ^{1}H NMR. Since Zn-salphen complexes have the tendency to form dimers or aggregate in non-coordinating solvents[71–73], DOSY NMR experiments were first performed to have a better insight into the nature of the tweezers in solution at the concentration of the catalysis experiments. Model Zn-salphen complex **9** presents a diffusion coefficient of 9.0×10^{-10} $m^2 \cdot s^{-1}$ in CD_2Cl_2 at 1.4 mM and 6 mM. In the presence of 5% THF the diffusion coefficient remains unchanged (9.0×10^{-10} $m^2 \cdot s^{-1}$) and the estimated molecular mass (593 ± 53 $g.mol^{-1}$) obtained using internal calibration by comparison with the diffusion coefficient of THF[76] is in agreement with a monomeric species (604 $g.mol^{-1}$) in solution under the conditions of the catalytic experiments. The diffusion coefficients of the open and closed tweezers of 5.8 and 5.4 × 10^{-10} $m^2 \cdot s^{-1}$ at 0.7 mM in CD_2Cl_2 THF (95/5) are also in agreement with monomeric species in solution (see Supplementary Table 3). The addition of 2-pyridinemethanol results in a slight decrease in the diffusion coefficient for both species as expected from the coordination to the Zn moieties and slight increase in size. It should be noted that the effect is more important for the open form than for the closed tweezers where the potential coordination inside the cavity affects less its hydrodynamic radius.

Reaction of 2-pyridinemethanol substrate with acetic anhydride was first investigated. Open tweezers **1** presented a significant increase in the initial reaction rate (0.50 $mM \cdot h^{-1}$) compared to uncatalyzed conditions where no reaction was detected (Fig. 5). This can be rationalized by a Lewis-acid activation of the anhydride. Interestingly, upon tweezers' closing

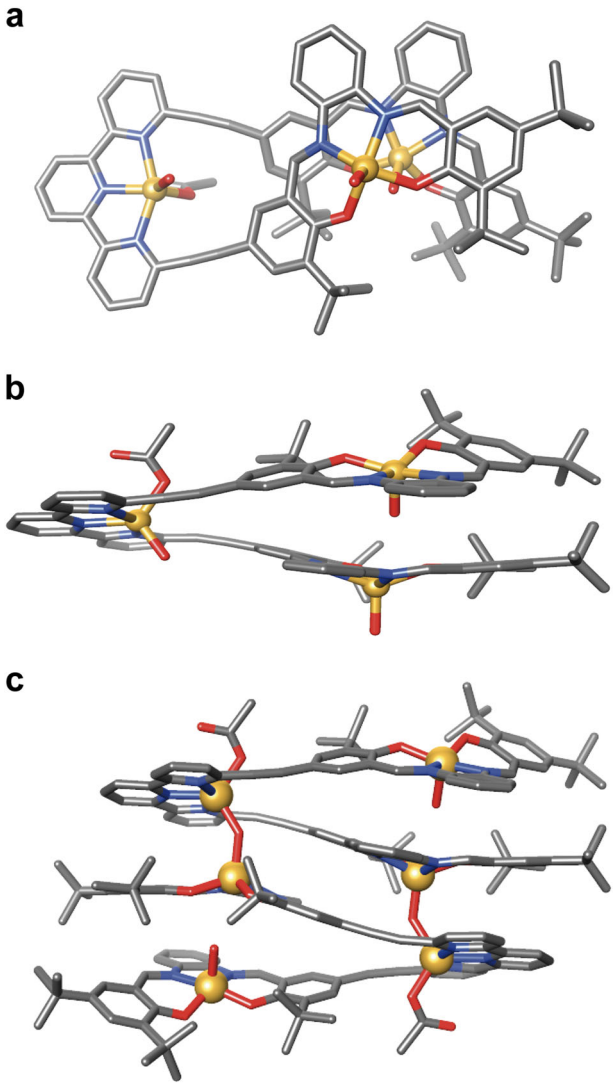

Fig. 3 Crystallographic structure of closed tweezers $[Zn(1)]^{2+}$. a top and **b** side view of the asymmetric unit; **c** dimeric structure. Solvent molecules and hydrogen atoms are omitted for clarity.

by $ZnCl_2$, a 13-fold increase of the initial rate was observed (6.6 mM·h^{-1}, Supplementary Table 4), providing initial evidence of an allosteric regulation of the acyl-transfer reaction. A control experiment performed with [Zn(terpy)Cl_2] complex presented some activity but with a significantly lower rate (0.24 mM·h^{-1}) compared to the open tweezers (Fig. 5) suggesting that the Zn(terpy)Cl_2 moiety doesn't play a significant role in the increase of activity. Another control experiment performed with Zn-salphen (at 28 mol% to have the same amount of Zn complex in solution as for open tweezers) presented an intermediate initial rate (1.9 mM h^{-1}) between that of open and closed tweezers. The reaction order in catalyst determined by the Burés graphical method[77,78] (see Supplementary Fig. 21) is first-order in Zn-salphen and also in open tweezers as expected for a monometallic activation of the anhydride. The higher initial rate for Zn-salphen compared to open tweezers can then be explained by the doubled concentration of Zn-salphen and a higher rate constant. The origin of such difference in activity between Zn-salphen and open tweezers was further investigated with half-tweezers **11** (see Supplementary Fig. 13) bearing only one Zn-salphen unit to evaluate the potential effect of the free terpyridine unit. Half-tweezers **11** also presents a lower initial rate (0.38 mM·h^{-1}) than Zn-salphen **9** (1.1 mM·h^{-1} at 14 mol%) suggesting a reduction in the Lewis acidity of the Zn unit by conjugation through the alkyne spacer to the free terpyridine unit. Upon zinc coordination to the terpyridine unit to form [Zn(**11**)Cl_2] the initial rate (1.5 mM·h^{-1}) becomes similar to control Zn-salphen **9** indicating a restoration of activity of the Zn-salphen unit. As final control experiment, the mixture of [Zn(terpy)Cl_2] (at 14 mol%) and Zn-salphen **9** (at 28 mol%) showed an initial rate (2.6 mM·h^{-1}) inferior than closed tweezers [Zn(**1**)Cl_2] (6.6 mM·h^{-1}). This suggests that the effect of the closed tweezers is not only due to the Zn(terpy)Cl_2 moiety in the closed tweezers but to the proximity in the cavity between both reagents, which enhances the reaction rate by decreasing the entropy of activation.

The effect of the anhydride on the allosteric regulation was also investigated using benzoic and trimethylacetic anhydrides (Fig. 15). Upon increasing the steric hindrance of the anhydride, the allosteric ratios were decreased (to 4 and 2-fold with Bz_2O and $(tBuCO)_2O$, respectively) which is in agreement with the reaction occurring in the cavity for the closed tweezers and being sensitive to the size of the acyl source (see Supplementary Figs. 16, 17, Supplementary Table 4). Since anhydrides are weakly coordinated to Zn-salphen, acetylimidazole was also investigated as acylating agent to enhance the binding to the Zn-salphen moiety by coordination via the imidazole unit (Fig. 6). A remarkable 80-fold increase in the initial reaction rate was observed upon closing of the tweezers. By contrast, control [Zn(terpy)Cl_2] complex presented almost no catalytic activity clearly indicating that the presence of an additional Lewis acid Zn(II) ion in the closed tweezers doesn't significantly contribute to the increase of rate by directly catalyzing the reaction. By applying an analogy to Sanders explanations for his system, Zn(II) coordination to the terpy moiety enables the conformational change that bring in close proximity the two substrates and results in a decrease of the activation entropy. The conversion however reached a plateau for the closed tweezers after around 2 h due to imidazole product inhibition. Indeed NMR monitoring indicates a stronger binding to the Zn-salphen of the generated imidazole than both substrates. The binding constants were determined by ^{1}H NMR titration on Zn-salphen complex in THF-d_8 with a value of log$K = 1.6$; 2.1 and 3.3 for 2-pyridinemethanol, acetylimidazole and imidazole, respectively (see Supplementary Figs. 8–10). Capitalizing on the significant values of allosteric ratio for 2-pyridinemethanol and acetic anhydride or acetylimidazole, *in situ* switching experiments were performed. Starting from the open tweezers a significant rate increase was observed upon tweezers' closing for both systems (Fig. 7). Upon re-opening the rate decreased again demonstrating *in situ* modulation of catalytic activity by this stimuli-responsive mechanical machine.

To have a better insight into the allosteric regulation, *meta* and *para*-pyridinemethanol substrates were also studied. The absolute rates are clearly lower than with *ortho* substrate (0.04 and 0.02 vs 0.5 mM.h^{-1} with open tweezers **1**) as already observed by Mirkin in a similar system[60]. One possible explanation is that the *ortho* derivative can establish an intramolecular hydrogen bond between the OH group and the nitrogen of the pyridyl moiety that enhances its nucleophilicity compared to *meta* and *para* derivatives. The allosteric effect is surprisingly reversed for *meta* and *para* substrates compared to *ortho* with an increased rate upon opening of the tweezers by 4.0- and 3.4-fold, respectively (Fig. 8, Supplementary Table 5). This trend can be rationalized either by a cavity too small, not enabling the right positioning of the two substrates for a double activation resulting in high energy transient state, or by a substrate inhibition effect for the closed form. Indeed, the *meta* and *para* isomers could act as a bridging ligand between the two Zn-salphen of the cavity via nitrogen and

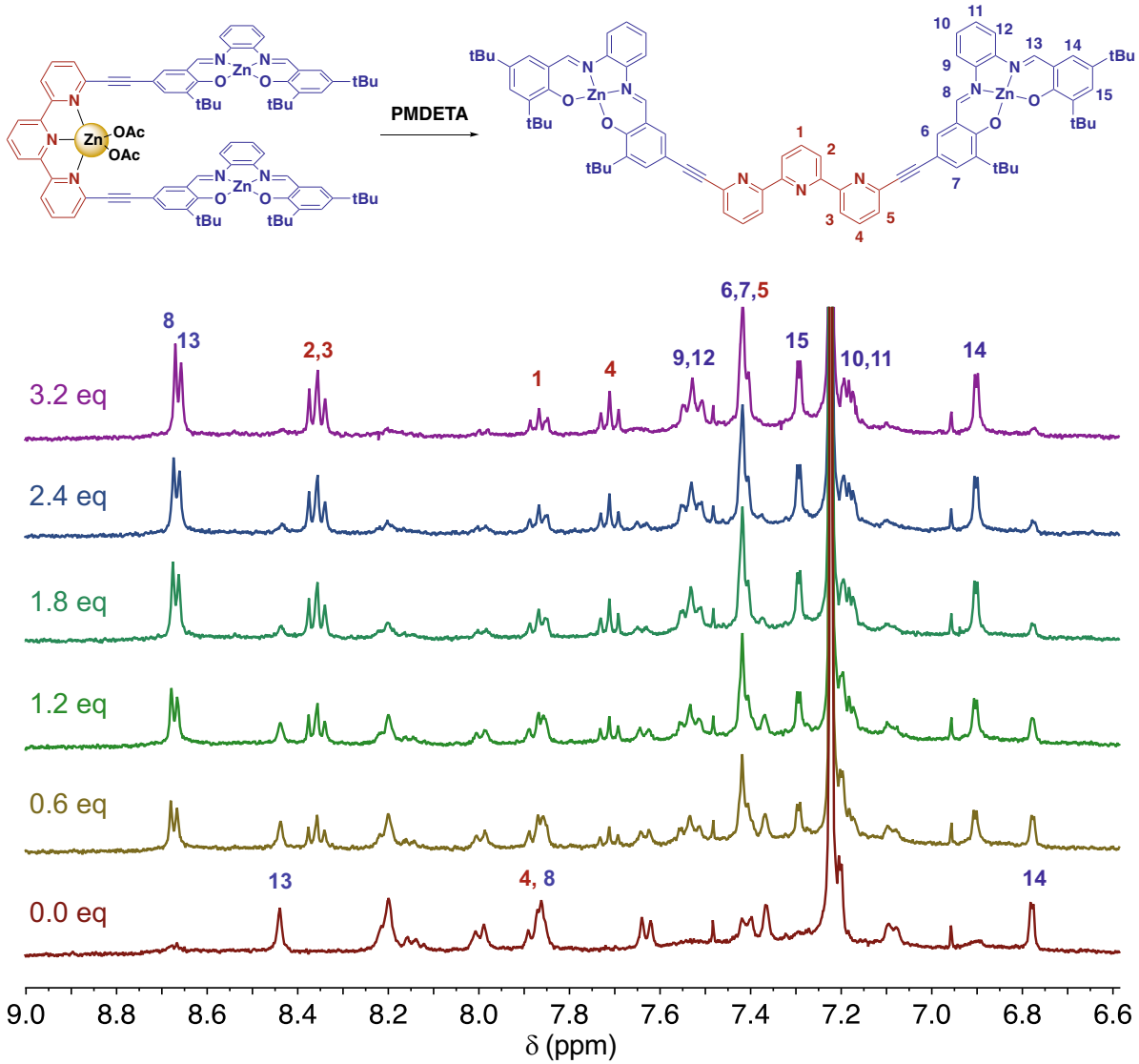

Fig. 4 Monitoring of the opening of [Zn(1)](OAc)$_2$ by ^{1}H NMR spectroscopy. ^{1}H NMR (400 MHz, $CDCl_3$ / CD_3OD (85/15), 300 K) titration of closed tweezers [Zn(**1**)](OAc)$_2$ (1.0×10^{-3} M) with PMDETA.

hydroxyl group coordination. The same reverse allosteric effect, albeit less pronounced (with 1.4 and 2.3-fold increase for *meta* and *para,* respectively), was also observed with acetylimidazole as acylating agent (see Supplementary Figs. 18, 19). These reduced allosteric ratios result from a relative increase of reactivity of the closed form compared to open one which is similar to the one with acetic anhydride. This trend is in favor of the substrate inhibition hypothesis as acetylimidazole can probably better compete than acetic anhydride with the bridging binding mode of *meta* or *para* substrates in the cavity due to its higher binding constant for Zn-salphen moieties allowing a double binding of acetylimidazole and substrate in the cavity.

The hypothesis of substrate inhibition by *meta* or *para* isomers was further supported by a competition experiment performed with closed tweezers and acetic anhydride in the presence of *ortho*, *meta* and *para* substrates in 1:1:1 ratio (see supplementary Fig. 20). In this case, almost no conversion was observed for 3- and 4-pyridinemethanol while the initial rate for 2-pyridinemethanol was clearly reduced (from 6.6 to 0.87 $mM{\cdot}h^{-1}$) as expected from a partial inhibition of the cavity by the binding of *meta* or *para* substrates. Thus, tweezers **1** present a remarkable substrate-dependent allosteric regulation with an up-regulation for *ortho* derivative and down regulation of *meta* and *para* upon closing. Such inversion in the allosteric response was not observed in the sandwich systems described by Mirkin which presented an up-regulation upon opening of the cavity for all three pyridinemethanol regioisomers. This points out the interest of these molecular tweezers architecture that not only present an allosteric regulation but a substrate-dependent response between three regioisomers.

For further support of our hypothesis, ^{1}H NMR titrations of closed tweezers were performed with 3- or 4-pyridinemethanol in $CDCl_3$/MeOD (85:15). Fittings of both binding isotherms are in agreement with the formation of 1:1 host/guest complexes with binding constants of $\log K = 3.9$ and 3.2 for *meta* and *para,* respectively (see Supplementary Figs. 11, 12). Variable temperature NMR experiments were performed in order to switch from a fast to a slow exchange regime. However, no coalescence was observed down to 220 K in both cases precluding NOESY experiments to assess the position of the substrate in the cavity. Since single crystals of suitable quality for diffraction studies could not be obtained, DFT calculations were performed to evaluate the geometry of *meta* and *para* substrates in the cavity. Due to the free rotation around the alkyne bonds the Zn-salphen moieties can adopt *syn* or *anti*

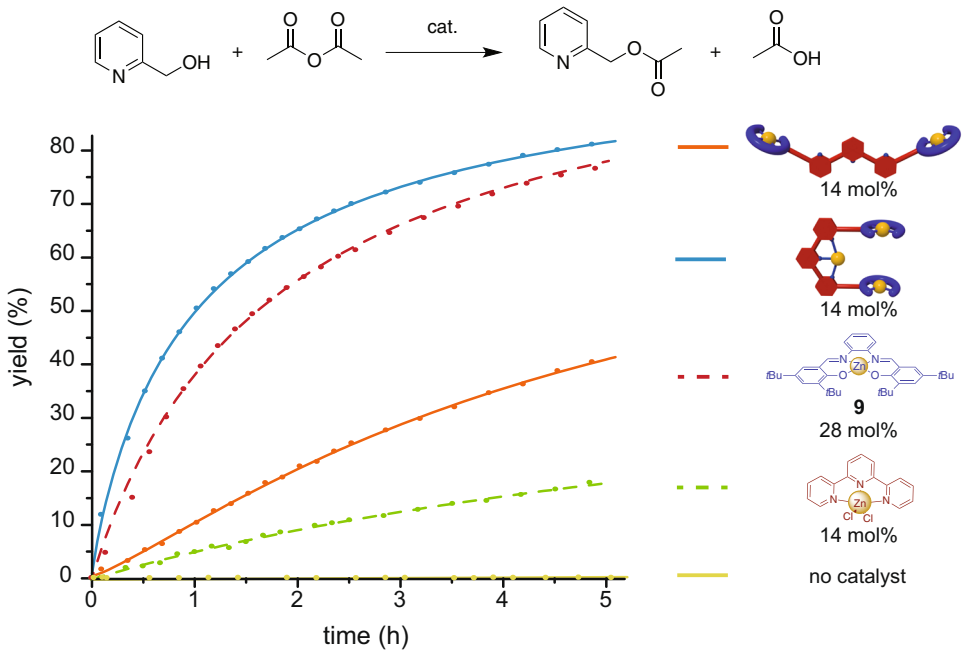

Fig. 5 Product (2-acetoxymethylpyridine) formation by the acyl-transfer reaction. The reaction was monitored by ^{1}H NMR under the following conditions: 2-pyridinemethanol (5 mM), acetic anhydride (5 mM), catalyst, CD_2Cl_2/THF-d_8 (95/5), 300 K; orange, open tweezers **1** (0.7 mM, 14 mol%); blue, closed tweezers [Zn(**1**)Cl_2] (0.7 mM, 14 mol%); red, Zn-salphen **9** (1.4 mM, 28 mol%); green [Zn(terpy)Cl_2] (0.7 mM, 14 mol%); yellow uncatalyzed.

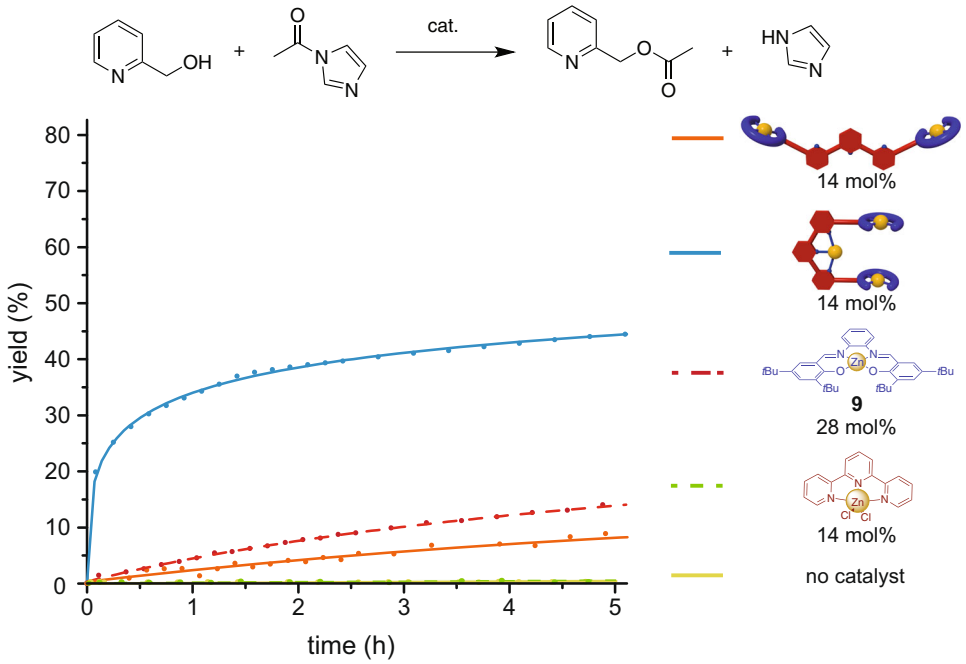

Fig. 6 Product (2-acetoxymethylpyridine) formation by the acyl-transfer reaction. The reaction was monitored by ^{1}H NMR with the following conditions: 2-pyridinemethanol (5 mM), acetylimidazole (5 mM), catalyst, CD_2Cl_2/THF-d_8 (95/5), 300 K; orange, open tweezers **1** (0.7 mM, 14 mol%); blue, closed tweezers [Zn(**1**)Cl_2] (0.7 mM, 14 mol%); red, Zn-salphen **9** (1.4 mM, 28 mol%); green [Zn(terpy)Cl_2] (0.7 mM, 14 mol%); yellow uncatalyzed.

conformations. Calculations were performed with both conformations resulting in similar geometries of the substrate bound inside the cavity (see Fig. 9 and Supplementary Fig. 22). The optimized geometries are compatible with bridged substrate complexes through coordination by the nitrogen atom of the pyridine and the oxygen of the hydroxyl group (Fig. 9c, d). The flexibility of the alkyne spacers enables a Zn–Zn distance of 8.06 and 8.61 Å for 3- and 4-pyridinemethanol, respectively. DFT calculations were also performed to model the active site of the closed tweezers in the presence of 2-pyridinemethanol (Fig. 9a, b) and acetic anhydride or acetylimidazole. The geometry of the reaction intermediate resulting from the addition of the hydroxyl group of 2-pyridinemethanol to the acetyl was optimized and is in agreement with the doubly bound tetrahedral intermediate proposed by Sanders[59]. The closed tweezers accommodates both substrates with Zn–Zn distances of 7.28 and 7.99 Å for acetic anhydride and acetylimidazole, respectively, which are comparable to the ones observed for the bridged *meta* and *para* derivatives in the cavity. The spatial

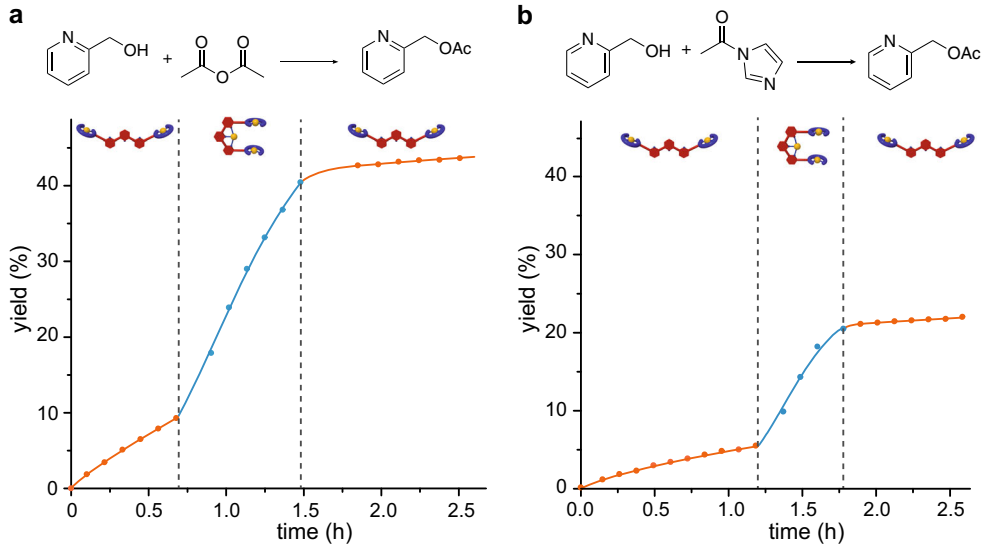

Fig. 7 Product (2-acetoxymethylpyridine) formation by the acyl-transfer reaction upon *in situ* switching. a Reaction with acetic anhydride and **b** with acetylimidazole. The reaction was monitored by ^{1}H NMR under the following conditions: 2-pyridinemethanol (5 mM), acyl derivative (5 mM), tweezers (0.7 mM, 14 mol%) in CD_2Cl_2/THF-d_8 (95/5), 300 K.

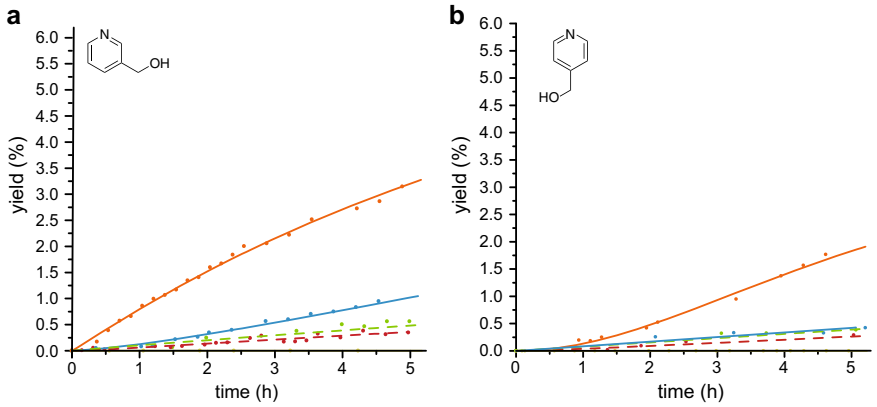

Fig. 8 Product formation by the acyl-transfer reaction with *meta* and *para* substrates. Product **a** 3-acetoxymethylpyridine and **b** 4-acetoxymethylpyridine The reaction was monitored by ^{1}H NMR under the following conditions: pyridinemethanol substrate (5 mM), acetic anhydride (5 mM), catalyst, CD_2Cl_2/THF-d_8 (95/5), 300 K; orange, open tweezers **1** (0.7 mM, 14 mol%); blue, closed tweezers [Zn(**1**)Cl_2] (0.7 mM, 14 mol%); red, Zn-salphen **9** (1.4 mM, 28 mol%); green [Zn(terpy)Cl_2] (0.7 mM, 14 mol%); yellow uncatalyzed.

proximity between both reagents in the closed conformation allows a cooperative effect that reduces the entropy of activation by transitioning from a bimolecular reaction in the open conformation to an intramolecular reaction. Thus, the experimental results and the DFT calculations all support our hypothesis of a cooperative bimetallic mechanism in the closed form for *ortho* substrate and an inhibition of the cavity for *meta* and *para* substrates.

In summary, switchable molecular tweezers incorporating two active Zn-salphen moieties have been obtained by a templated synthesis approach. The tweezers were reversibly switched between an open and a closed form by a coordination stimulus changing drastically the intramolecular distance between the two Zn-salphen moieties. Such mechanical motion was exploited to obtain an allosteric regulation in acyl-transfer reactions as a proof of principle. Indeed, a significant increase in rate was observed for 2-pyridinemethanol substrate upon closing due to the spatial proximity in the cavity between this substrate and acetic anhydride. Upon screening acylating agents, acetylimidazole proved to be the reagent with the highest allosteric regulation effect with an 80-fold increase in rate upon tweezers' closing. Remarkably, our system displays a substrate dependent allosteric response, as for 3- and 4-pyridinemethanol substrates a down regulation is observed upon closing. This decrease of the rate of reaction was rationalized by a substrate inhibition in the closed form via an intramolecular bridging that blocks the active site. In conclusion, the mechanical motion of the tweezers enabled a remarkable substrate-dependent allosteric response in a benchmark acyl-transfer reaction that opens new perspectives for regulating other cooperative catalytic reactions.

Methods

Synthetic procedures. See supplementary methods and Supplementary Figs. 23–41.

XRD crystal structures. See Supplementary Fig. 1 and Supplementary Tables 1, 2 for selected XRD data. Crystallographic information files for Zn(**1**)$(OAc)_2$ and Zn(**1**)$(OAc_{0.25}/Cl_{0.75})_2$ are provided in Supplementary Data 1, 2, respectively.

Characterization of the compounds. See Supplementary Figs. 2, 3 and Supplementary Figs. 23–41 for NMR spectra. See Supplementary Figs. 6, 7 for HRMS spectra. See Supplementary Table 3 for diffusion coefficients.

Switching and binding studies. See Supplementary Figs. 4, 5 for UV–Vis and NMR titrations. See Supplementary Figs. 8–12 for binding NMR titrations.

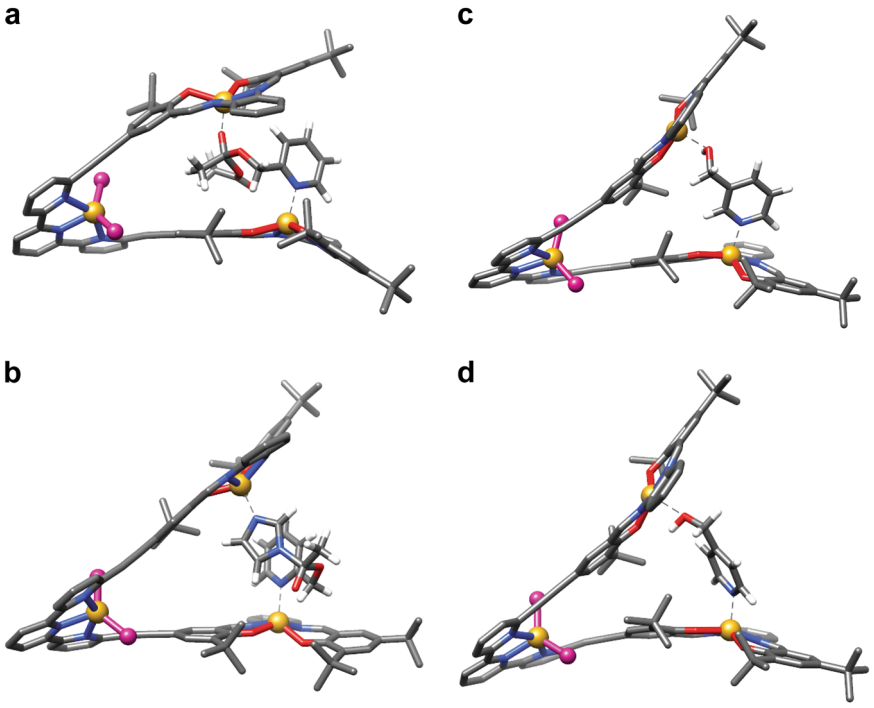

Fig. 9 DFT optimized geometries. a tetrahedral intermediate doubly bound inside the cavity of *anti*-closed tweezers [Zn(**1**)Cl_2] with 2-pyridinemethanol and acetic anhydride. **b** *anti*-closed tweezers [Zn(**1**)Cl_2] with 2-pyridinemethanol and acetylimidazole. **c** bridging 3-pyridinemethanol substrate in the cavity of *anti*-closed tweezers [Zn(**1**)Cl_2]. **d** bridging 4-pyridinemethanol substrate in the cavity of *anti*-closed tweezers [Zn(**1**)Cl_2]. DFT calculations were carried out at (M06/6-311 G**) level.

Catalysis experiments. See Supplementary Figs. 13–20 and Supplementary Tables 4–6 for all control experiments. See Supplementary Fig. 21 for kinetics analysis.

DFT modeling. See Supplementary Fig. 22 and Supplementary Tables 7–13 for optimized coordinates.

Data availability

The authors declare that all data supporting the findings of this study are available within the article and Supplementary Information files, and also from the corresponding author upon reasonable request. The X-ray crystallographic coordinates for the structures reported in this article have been deposited at the Cambridge Crystallographic Data Centre (CCDC), under deposition numbers CCDC 1872042 and 1872043. These data can be obtained free of charge from The Cambridge Crystallographic Data Centre at www.ccdc.cam.ac.uk/data_request/cif.

Received: 20 June 2019; Accepted: 28 November 2019;
Published online: 20 December 2019

References

1. Kay, E. R., Leigh, D. A. & Zerbetto, F. Synthetic molecular motors and mechanical machines. *Angew. Chem. Int. Ed.* **46**, 72–191 (2007).
2. Balzani, V., Venturi, M. & Credi, A. *Molecular Devices and Machines: Concepts and Perspectives for the Nanoworld* (Wiley-VCH, Weinheim, 2008).
3. Erbas-Cakmak, S., Leigh, D. A., McTernan, C. T. & Nussbaumer, A. L. Artificial molecular machines. *Chem. Rev.* **115**, 10081–10206 (2015).
4. Browne, W. R. & Feringa, B. L. *Molecular Switches* (Wiley-VHC, 2011).
5. Eelkema, R. et al. Molecular machines: Nanomotor rotates microscale objects. *Nature* **440**, 163–163 (2006).
6. Vives, G. & Tour, J. M. Synthesis of single-molecule nanocars. *Acc. Chem. Res.* **42**, 473–487 (2009).
7. Perera, U. G. E. et al. Controlled clockwise and anticlockwise rotational switching of amolecular motor. *Nat. Nanotechnol.* **8**, 46–51 (2013).
8. Kudernac, T. et al. Electrically driven directional motion of a four-wheeled molecule on a metal surface. *Nature* **479**, 208–211 (2011).
9. Lewandowski, B. et al. Sequence-specific peptide synthesis by an artificial small-molecule machine. *Science* **339**, 189–193 (2013).
10. Zigon, N., Guenet, A., Graf, E. & Hosseini, M. W. A platinum based organometallic turnstile. *Chem. Commun.* **49**, 3637–3639 (2013).
11. Lüning, U. Switchable catalysis. *Angew. Chem. Int. Ed.* **51**, 8163–8165 (2012).
12. Wiester, M. J., Ulmann, P. A. & Mirkin, C. A. Enzyme mimics based upon supramolecular coordination chemistry. *Angew. Chem. Int. Ed.* **50**, 114–137 (2011).
13. Neilson, B. M. & Bielawski, C. W. Illuminating photoswitchable catalysis. *ACS. Catalysis* **3**, 1874–1885 (2013).
14. Blanco, V., Leigh, D. A. & Marcos, V. Artificial switchable catalysts. *Chem. Soc. Rev.* **44**, 5341–5370 (2015).
15. van Dijk, L. et al. Molecular machines for catalysis. *Nat. Rev. Chem.* **2**, 0117 (2018).
16. Peters, M. V., Stoll, R. S., Kühn, A. & Hecht, S. Photoswitching of basicity. *Angew. Chem. Int. Ed.* **47**, 5968–5972 (2008).
17. Berryman, O. B., Sather, A. C., Lledó, A. & Rebek, J. Switchable catalysis with a light-responsive cavitand. *Angew. Chem. Int. Ed.* **50**, 9400–9403 (2011).
18. Berryman, O. B., Sather, A. C., Lledó, A. & Rebek, J. Switchable catalysis with a light-responsive cavitand. *Angew. Chem. Int. Ed.* **50**, 9400–9403 (2011).
19. Cacciapaglia, R., Di Stefano, S. & Mandolini, L. The bis–barium complex of a butterfly crown ether as a phototunable supramolecular catalyst. *J. Am. Chem. Soc.* **125**, 2224–2227 (2003).
20. Neilson, B. M. & Bielawski, C. W. Photoswitchable organocatalysis: using light to modulate the catalytic activities of N-heterocyclic carbenes. *J. Am. Chem. Soc.* **134**, 12693–12699 (2012).
21. Wang, J. & Feringa, B. L. Dynamic control of chiral space in a catalytic asymmetric reaction using a molecular motor. *Science* **331**, 1429–1432 (2011).
22. Vlatkovic, M., Bernardi, L., Otten, E. & Feringa, B. L. Dual stereocontrol over the Henry reaction using a light- and heat-triggered organocatalyst. *Chem. Commun.* **50**, 7773–7775 (2014).
23. Blanco, V., Carlone, A., Hänni, K. D., Leigh, D. A. & Lewandowski, B. A rotaxane-based switchable organocatalyst. *Angew. Chem. Int. Ed.* **51**, 5166–5169 (2012).
24. Blanco, V., Leigh, D. A., Marcos, V., Morales-Serna, J. A. & Nussbaumer, A. L. A switchable [2]rotaxane asymmetric organocatalyst that utilizes an acyclic chiral secondary amine. *J. Am. Chem. Soc.* **136**, 4905–4908 (2014).
25. Beswick, J. et al. Selecting reactions and reactants using a switchable rotaxane organocatalyst with two different active sites. *Chem. Sci.* **6**, 140–143 (2015).
26. Galli, M., Lewis, J. E. M. & Goldup, S. M. A stimuli-responsive rotaxane–gold catalyst: regulation of activity and diastereoselectivity. *Angew. Chem. Int. Ed.* **54**, 13545–13549 (2015).

27. Centola, M., Valero, J. & Famulok, M. Allosteric control of oxidative catalysis by a DNA rotaxane nanostructure. *J. Am. Chem. Soc.* **139**, 16044–16047 (2017).
28. Marcos, V. et al. Allosteric initiation and regulation of catalysis with a molecular knot. *Science* **352**, 1555–1559 (2016).
29. Petitjean, A., Kyritsakas, N. & Lehn, J. M. Ion-triggered multistate molecular switching device based on regioselective coordination-controlled ion binding. *Chem. Eur. J.* **11**, 6818–6828 (2005).
30. McConnell, A. J., Wood, C. S., Neelakandan, P. P. & Nitschke, J. R. Stimuli-responsive metal–ligand assemblies. *Chem. Rev.* **115**, 7729–7793 (2015).
31. Machan, C. W. et al. One-pot synthesis of an Fe(II) bis–terpyridine complex with allosterically regulated electronic properties. *J. Am. Chem. Soc.* **134**, 16921–16924 (2012).
32. Lifschitz, A. M. et al. An allosteric photoredox catalyst inspired by photosynthetic machinery. *Nat. Commun.* **6**, 6541 (2015).
33. Lifschitz, A. M., Rosen, M. S., McGuirk, C. M. & Mirkin, C. A. Allosteric supramolecular coordination constructs. *J. Am. Chem. Soc.* **137**, 7252–7261 (2015).
34. Fermi, A., Bergamini, G., Roy, M., Gingras, M. & Ceroni, P. Turn-on Phosphorescence by metal coordination to a multivalent terpyridine ligand: a new paradigm for luminescent sensors. *J. Am. Chem. Soc.* **136**, 6395–6400 (2014).
35. Park, K. M., Murray, J. & Kim, K. Ultrastable artificial binding pairs as a supramolecular latching system: a next generation chemical tool for proteomics. *Acc. Chem. Res.* **50**, 644–646 (2017).
36. Schmittel, M., De, S. & Pramanik, S. Reversible ON/OFF nanoswitch for organocatalysis: mimicking the locking and unlocking operation of CaMKII. *Angew. Chem. Int. Ed.* **51**, 3832–3836 (2012).
37. De, S., Pramanik, S. & Schmittel, M. A toggle nanoswitch alternately controlling two catalytic reactions. *Angew. Chem. Int. Ed.* **53**, 14255–14259 (2014).
38. Ouyang, G. H., He, Y. M., Li, Y., Xiang, J. F. & Fan, Q. H. Cation-triggered switchable asymmetric catalysis with chiral Aza-CrownPhos. *Angew. Chem. Int. Ed.* **54**, 4334–4337 (2015).
39. Vidal-Ferran, A., Mon, I., Bauzá, A., Frontera, A. & Rovira, L. Supramolecularly regulated ligands for asymmetric hydroformylations and hydrogenations. *Chem. Eur. J.* **21**, 11417–11426 (2015).
40. Vaquero, M., Rovira, L. & Vidal-Ferran, A. Supramolecularly fine-regulated enantioselective catalysts. *Chem. Commun.* **52**, 11038–11051 (2016).
41. Mittal, N., Pramanik, S., Paul, I., De, S. & Schmittel, M. Networking nanoswitches for ON/OFF control of catalysis. *J. Am. Chem. Soc.* **139**, 4270–4273 (2017).
42. Ouyang, G.-H., He, Y.-M. & Fan, Q.-H. Podand-based dimeric chromium (III)–salen complex for asymmetric henry reaction: cooperative catalysis promoted by complexation of alkali metal ions. *Chem. Eur. J.* **20**, 16454–16457 (2014).
43. Oliveri, C. G., Ulmann, P. A., Wiester, M. J. & Mirkin, C. A. Heteroligated supramolecular coordination complexes formed via the halide-induced ligand rearrangement reaction. *Acc. Chem. Res.* **41**, 1618–1629 (2008).
44. Gianneschi, N. C. et al. A supramolecular approach to an allosteric catalyst. *J. Am. Chem. Soc.* **125**, 10508–10509 (2003).
45. Gianneschi, N. C., Cho, S.-H., Nguyen, S. T. & Mirkin, C. A. Reversibly addressing an allosteric catalyst in situ: catalytic molecular tweezers. *Angew. Chem. Int. Ed.* **43**, 5503–5507 (2004).
46. Gianneschi, N. C., Nguyen, S. T. & Mirkin, C. A. Signal amplification and detection via a supramolecular allosteric catalyst. *J. Am. Chem. Soc.* **127**, 1644–1645 (2005).
47. Yoon, H. J., Kuwabara, J., Kim, J.-H. & Mirkin, C. A. Allosteric supramolecular triple-layer catalysts. *Science* **330**, 66–69 (2010).
48. Raynal, M., Ballester, P., Vidal-Ferran, A. & van Leeuwen, P. W. N. M. Supramolecular catalysis. Part 2: artificial enzyme mimics. *Chem. Soc. Rev.* **43**, 1734–1787 (2014).
49. Leblond, J. & Petitjean, A. Molecular tweezers: concepts and applications. *ChemPhysChem* **12**, 1043–1051 (2011).
50. Hardouin-Lerouge, M., Hudhomme, P. & Salle, M. Molecular clips and tweezers hosting neutral guests. *Chem. Soc. Rev.* **40**, 30–43 (2011).
51. Klärner, F.-G. & Kahlert, B. Molecular tweezers and clips as synthetic receptors. molecular recognition and dynamics in receptor−substrate complexes. *Acc. Chem. Res.* **36**, 919–932 (2003).
52. Zimmerman, S. Rigid molecular tweezers as hosts for the complexation of neutral guests. *Top. Curr. Chem.* **165**, 71–102 (1993).
53. Doistau, B. et al. Switchable platinum-based tweezers with Pt–Pt bonding and selective luminescence quenching. *Dalton Trans.* **44**, 8543–8551 (2015).
54. Doistau, B. et al. Terpy(Pt–salphen)2 switchable luminescent molecular tweezers. *Chem. Eur. J.* **20**, 15799–15807 (2014).
55. Benda, L., Doistau, B., Hasenknopf, B. & Vives, G. Synthesis and guest recognition of switchable Pt-salphen based molecular tweezers. *Molecules* **23**, 990 (2018).
56. Doistau, B. et al. Mechanical switching of magnetic interaction by tweezers-type complex. *Chem. Commun.* **51**, 12916–12919 (2015).
57. Doistau, B., Benda, L., Hasenknopf, B., Marvaud, V. & Vives, G. Switching magnetic properties by a mechanical motion. *Magnetochemistry* **4**, 5 (2018).
58. Doistau, B. et al. Six states switching of redox-active molecular tweezers by three orthogonal stimuli. *J. Am. Chem. Soc.* **139**, 9213–9220 (2017).
59. Mackay, L. G., Wylie, R. S. & Sanders, J. K. M. Catalytic acyl transfer by a cyclic porphyrin trimer: efficient turnover without product inhibition. *J. Am. Chem. Soc.* **116**, 3141–3142 (1994).
60. Masar, M. S. et al. Allosterically regulated supramolecular catalysis of acyl transfer reactions for signal amplification and detection of small molecules. *J. Am. Chem. Soc.* **129**, 10149–10158 (2007).
61. Oliveri, C. G. et al. Supramolecular allosteric cofacial porphyrin complexes. *J. Am. Chem. Soc.* **128**, 16286–16296 (2006).
62. Kleij, A. W., Tooke, D. M., Spek, A. L. & Reek, J. N. H. A convenient synthetic route for the preparation of nonsymmetric metallo-salphen complexes. *Eur. J. Inorg. Chem.* **2005**, 4626–4634 (2005).
63. Kleij, A. W. Nonsymmetrical salen ligands and their complexes: synthesis and applications. *Eur. J. Inorg. Chem.* **2009**, 193–205 (2009).
64. Muñoz-Hernández, M.-A., Keizer, T. S., Parkin, S., Patrick, B. & Atwood, D. A. Group 13 cation formation with a potentially tridentate ligand. *Organometallics* **19**, 4416–4421 (2000).
65. Song, F. et al. (R,R)-salen/salan-based polymer fluorescence sensors for Zn2+ detection. *Polymer* **52**, 6029–6036 (2011).
66. Sellner, H., Karjalainen, J. K. & Seebach, D. Preparation of dendritic and non-dendritic styryl-substituted salens for cross-linking suspension copolymerization with styrene and multiple use of the corresponding Mn and Cr complexes in enantioselective epoxidations and hetero-Diels–Alder reactions. *Chem. Eur. J.* **7**, 2873–2887 (2001).
67. Holbach, M. & Weck, M. Modular approach for the development of supported, monofunctionalized, salen catalysts. *J. Org. Chem.* **71**, 1825–1836 (2006).
68. Singer, A. L. & Atwood, D. A. Five-coordinate Salen(tBu) complexes of zinc. *Inorg. Chim. Acta* **277**, 157–162 (1998).
69. Escudero-Adán, E. C., Benet-Buchholz, J. & Kleij, A. W. Trapping of a four-coordinate zinc salphen complex inside a crystal matrix. *Chem. Eur. J.* **15**, 4233–4237 (2009).
70. Decortes, A., Martinez Belmonte, M., Benet-Buchholz, J. & Kleij, A. W. Efficient carbonate synthesis under mild conditions through cycloaddition of carbon dioxide to oxiranes using a Zn(salphen) catalyst. *Chem. Commun.* **46**, 4580–4582 (2010).
71. Consiglio, G., Failla, S., Finocchiaro, P., Oliveri, I. P. & Di Bella, S. An unprecedented structural interconversion in solution of aggregate Zinc(II) salen Schiff-base complexes. *Inorg. Chem.* **51**, 8409–8418 (2012).
72. Forte, G., Oliveri, I. P., Consiglio, G., Failla, S. & Di Bella, S. On the Lewis acidic character of bis(salicylaldiminato)zinc(ii) Schiff-base complexes: a computational and experimental investigation on a series of compounds varying the bridging diimine. *Dalton Trans.* **46**, 4571–4581 (2017).
73. Kleij, A. W. et al. Supramolecular zinc(II)salphen motifs: Reversible dimerization and templated dimeric structures. *Inorg. Chim. Acta* **359**, 1807–1814 (2006).
74. Zelder, F. H. & Rebek Jr, J. Cavitand templated catalysis of acetylcholine. *Chem. Commun*. 753–754 (2006).
75. Deria, P. et al. Framework-topology-dependent catalytic activity of zirconium-based (porphinato)zinc(II) MOFs. *J. Am. Chem. Soc.* **138**, 14449–14457 (2016).
76. Neufeld, R. & Stalke, D. Accurate molecular weight determination of small molecules via DOSY-NMR by using external calibration curves with normalized diffusion coefficients. *Chem. Sci.* **6**, 3354–3364 (2015).
77. Burés, J. A simple graphical method to determine the order in catalyst. *Angew. Chem. Int. Ed.* **55**, 2028–2031 (2016).
78. Nielsen, C. D. T. & Burés, J. Visual kinetic analysis. *Chem. Sci.* **10**, 348–353 (2019).

Acknowledgements

B.D. thanks the Ecole Normale Supérieure de Cachan for a PhD Fellowship. Dr Valérie Marvaud (SU) is warmly acknowledged for fruitful discussions. Financial support from the ANR SMARTEES (15-CE07–0006–01), CNRS and Sorbonne University are acknowledged.

Author contributions

G.V. and L.B. conceived and designed the experiments. L.B., B.D., and C.R.-G. carried out the experimental work, analysis and interpretation of the results. L.-M.C. resolved the crystallographic structures. B.H. supported and supervised the project. G.V. supervised the project and supported the analysis and interpretation of the results. All authors discussed the results and edited the manuscript.

Competing interests
The authors declare no competing interests.

Additional information
Supplementary information is available for this paper at https://doi.org/10.1038/s42004-019-0246-9.

Correspondence and requests for materials should be addressed to G.V.

Reprints and permission information is available at http://www.nature.com/reprints

Publisher's note Springer Nature remains neutral with regard to jurisdictional claims in published maps and institutional affiliations.